Coated Semiconductor Nanoparticles: The CdS/PbS System's Photoluminescence Properties

H. S. Zhou,*,† H. Sasahara, I. Honma, and H. Komiyama

The Department of Chemical Engineering, Faculty of Engineering, The University of Tokyo, Bunkyo-ku, Tokyo, 113, Japan

Joseph W. Haus

The Department of Physics, Rensselaer Polytechnic Institute, Troy, New York 12180-3590

Received January 24, 1994. Revised Manuscript Received May 16, 1994®

The photoluminescence (PL) spectra from colloidal solution of coated semiconductor CdS/PbS nanoparticles, which are synthesized by a cation-exchanging colloidal method, are measured at room temperature. The PL spectra from S vacancies (V_S) and Cd–S composite vacancies (V_{Cd-S}) in CdS and CdS/PbS nanoparticles have been investigated. The PL of V_S can be quenched only by the Pb caption modified in the surface of CdS. The PL of V_{Cd-S} in CdS nanoparticles appears in about 1100 nm. The PL of V_{Cd-S} in CdS/PbS nanoparticles shifts to longer wavelengths as the quantity of PbS increases. The shift and intensity variation of the PL peak from V_{Cd-S} in CdS/PbS can be explained by a quantum confinement model of coated nanoparticles; the excited energy gap (HOMO–LUMO) is not only dependent on the size of the particles but also strongly dependent on the core/shell ratio of the coated nanoparticles. The PL energy gap (LUMO–V_{Cd-S}) is also strongly dependent on the core/shell ratio.

Introduction

Special attention has been devoted to nanometer-size particles because of their large size-dependent properties. Due to the spatial confinement of the photogenerated charge carriers, the electronic levels shift to higher energies. The interest in these heterogeneous materials has been primarily motivated by their fundamental quantum properties,[1–8] especially optical properties which include absorption spectra, nonlinear optical response,[9,10] Raman spectra,[1,11] and photoluminescence (PL).[12,13] The nanometer-size semiconductor particles have been fabricated by a wide variety of methods,[14,15] including colloidal solutions, zeolite structures, sputtering, and doping in Vycor glasses.

Recently, research results on heterogeneous or coated semiconductor nanoparticles have been reported and reviewed;[16] examples include CdS/AgI,[17] CdS/TiO_2,[17] AGI/Ag_2S,[18] ZnS/CdSe,[5] ZnSe/CdSe,[19] and CdS/PbS.[20] Some optical properties and band structure models of them have also been investigated.

We have reported a synthesis and some properties of the coated nanoparticles CdS/PbS system.[20] In this paper, we first explore the infrared PL emission of CdS resulted from the Cd–S composite vacancies; we then explore the PL of the coated nanoparticles CdS/PbS system. The PL spectra of CdS particles have been investigated by several groups;[12,21] there are two PL peaks, one near the violet spectral regime results from electron–hole pair recombination across the bandgap and the other one in the red spectral regime is due to the recombination of a electron, trapped in a sulfur vacancy, with a hole in the valence band of CdS nanoparticles.[22,23]

† Present address: Nano-Photonics Materials Lab, Frontier system, the Institute of Physical and Chemical Research (RIKEN), Hirosawa 2-1, Wako-shi, Saitama, 351-01, Japan.

® Abstract published in *Advance ACS Abstracts,* July 1, 1994.

(1) Rosetti, R.; Nakahara, S.; Brus, L. E. *J. Chem. Phys.* **1983**, *79*, 1086–1088.
(2) Rosetti, R.; Ellison, J. L.; Gibson, J. M.; Brus, L. E. *J. Chem. Phys.* **1984**, *80*, 4464–4469.
(3) Fojtik, A.; Weller, H.; Koch, V.; Henglein, A. *Ber. Bunsenges. Phys. Chem.* **1984**, *88*, 969–977.
(4) Herron, N.; Wang, Y.; Eckert, H. *J. Am. Chem. Soc.* **1990**, *112*, 1322–1326.
(5) Kortan, A. R.; Hull, R.; Opila, R. L.; Bawendi, M. G.; Steigerwald, M. L.; Carroll, R. J.; Brus, L. E. *J. Am. Chem. Soc.* **1990**, *112*, 1327–1332.
(6) Zhao, X. K.; Fendler, J. H. *J. Phys. Chem.* **1991**, *95*, 3716–3723.
(7) Takagahara, T. *Phys. Rev. B* **1989**, *39*, 10206–10231.
(8) Kayanuma, T. *Phys. Rev. B* **1986**, *38*, 9797–9805.
(9) Jain, R. K.; Lind, R. C. *J. Opt. Soc. Am.* **1983**, *73*, 647–653.
(10) Roussignol, P.; Ricard, D.; Lukasik, J.; Flytzanis, C. *J. Opt. Soc. Am. B* **1987**, *4*, 5–13.
(11) Shiang, J. J.; Goldstein, A. N.; Alivisatos, A. P. *J. Chem. Phys.* **1990**, *92*, 3232–3233.
(12) Wang, Y.; Herron, N. *J. Phys. Chem.* **1988**, *92*, 4988–4994.
(13) Ramsden, J. J.; Webber, S. E.; Gratzel, M. *J. Phys. Chem.* **1985**, *89*, 2740–2743.
(14) Shinojima, H.; Yumoto, J.; Uesugi, N.; Omi, S.; Asahara, Y. *Appl. Phys. Lett.* **1989**, *55*, 1519–1521.
(15) Yumoto, Y.; Shinojima, H.; Uesugi, N.; Tsunetomo, K.; Nasu, H.; Osaka, Y. *Appl. Phys. Lett.* **1990**, *57*, 2393–2395.
(16) Henglein, A. *Chem. Rev.* **1989**, *89*, 1861–1873.
(17) Spanhel, L.; Weller, H.; Henglein, A. *J. Am. Chem. Soc.* **1987**, *109*, 6632–6635.
(18) Heinglein, A.; Gutierrez, M.; Weller, H.; Fojtik, A.; Jirkovsky, J. *Ber. Bunsen-Ges. Phys. Chem.* **1989**, *93*, 5578.
(19) Hoener, C. F.; Allan, K. A.; Bard, A. J.; Campion, A.; Fox, M. A.; Mallouk, T. E.; Webber, S. E.; White, J. M. *J. Phys. Chem.* **1992**, *96*, 3812–3817.
(20) Zhou, H. S.; Honma, I.; Komiyama, H.; Haus, J. W. *J. Phys. Chem.* **1993**, *97*, 895–901.
(21) Ishiwatari, T.; Komiyama, H., unpublished.
(22) Ramsden, J. J.; Gratzel, M. *J. Chem. Soc., Faraday Trans. 1* **1984**, *80*, 919–933.
(23) Kamat, P. V.; Dimitrijevic, M. N.; Fessenden, R. W. *J. Phys. Chem.* **1987**, *91*, 396–401.

0897-4756/94/2806-1534$04.50/0

The PL characteristics of the AgI/Ag_2S,[18] CdS/HgS,[34,35] and CdS/HgS/CdS[36] systems have been described. But, in these papers, the results were correlated with a quantized energy structure of the coated semiconductor particles. However, we explore both the shift and intensity variation of PL spectra in CdS/PbS system and then present a quantitative theoretical treatment.

In the CdS/PbS system, we find an infrared PL peak that is attributed to Cd–S composite vacancies at the interface between CdS and PbS. The peak shifts to longer wavelengths as the thickness of the PbS shell layer increases. This phenomenon can be explained by a quantum-confinement model of coated semiconductor nanoparticles; since bulk PbS material has a bandgap energy of 0.4 eV, compared to the CdS bandgap energy of 2.4 eV, the energy shift of carrier states decreases as the thickness of the PbS shell increases. The overlap of electron wave function with surface states is also strongly affected by the shell layer thickness.

Several qualitative reports have examined of the dynamics of electron–hole pair recombination of the CdS–Ag_2S[24] and AgI–Ag_2S[18] semiconductor–semiconductor sandwich structure nanoparticles.[16] These phenomena are qualitatively explained by a carrier-transfer mechanism between the two semiconductor materials. In this paper, we calculate the carrier wave functions to determine the amount of charge transfer betwen the two materials by a detailed model; this procedure is in the same spirit as treatments of superlattices in which the carriers find themselves in quantized subband states.[25] We discuss the PL spectra of the CdS/PbS system based on our model of quantum coherence between the core and shell layers. This approach is generally applicable and can be applied to other heterostructure particle systems with appropriate changes for the particle geometry and the material parameters.

Experiment

The fabrication and characteristic of the coated CdS/PbS nanoparticles have been discussed in detail in our previous paper.[20] Here we just present a short discussion of the synthesis method. Na_2S (10 cm^3, 4 mM) aqueous solution is injected to the mixture solution of $CdCl_2$ (10 cm^3, 5 mM) aqueous solution and 5% polyvenylpyrolydon (10 cm^3, PVP) aqueous solution to form CdS nanoparticles with about 60 Å diameter. These nanoparticles remain stable in the solution with the stabilizing agent PVP; it coats the CdS surface, which prevents the particles from coalescencing.

Then, $Pb(CH_3COO)_2$ aqueous solution is poured into above colloidal solution. The Pb^{2+} ion displaces Cd in the Cd–S bond to form a Pb–S bond and a PbS shell layer on the surface of CdS nanoparticles. The color of the coated semiconductor nanoparticles (CSN) solution changes within several minutes or several hours according to the concentration of $Pb(CH_3COO)_2$ in the solution. We use the Pb/Cd (the molar ratio of the $Pb(CH_3COO)_2$ to $CdCl_2$) to express the quantity of the $Pb(CH_3COO)_2$. All of the CdS nanoparticles would transform into PbS if the lead ion concentration were high enough and the time after the injection Pb^{2+} were long enough. The procedure of ion displacement can be expressed as

$$Pb^{2+} + CdS \rightleftharpoons Cd^{2+} + PbS + G$$

The reaction Gibbs energy G is identical to 4.618 K J/mol. From the phase diagram of the CdS-PbS solid solution, we deduce that the two solids are immiscible.[26] Here, we replace the $Cd(NO_3)_2$ and $Pb(NO_3)_2$ aqueous solution with the $CdCl_2$ and $Pb(CH_3COO)_2$ aqueous solution to avoid a possible oxidation reaction at the PbS surface in preparing the film.

The specimen for the PL measurement is prepared as follows: 5 min after the injection of Pb cations into the CdS particle solution, a droplet of the solution is dried on the Si substrate in a drier for about 5 min; thus a solid PVP film containing CdS/PbS microparticles is formed. The optical absorption measurements from the solution samples are also made at 5 min after the Pb cations are introduced into the solution. In this way, the measurement of absorption and PL data corresponds as closely as possible to particles with the same core/shell ratio.

PL studies are performed by exciting the sample at room temperature by an argon ion laser with the exciting wavelength 514.5 nm. The intensity of the laser is adjusted to 100 mW or lower. Under the higher excitation conditions, the PL of the nanoparticles show strong extinction with time (strong enough to be seen by eye).

Results and Discussion

Photoluminescence Spectra of CdS and PbS. In Figure 1 the PL and optical absorption spectra of the CdS nanoparticles are displayed. The CdS colloidal solution is prepared by a $CdCl_2$ solution (10 cm^3 5 mM) mixed with a Na_2S aqueous solution (10 cm^3 5 mM). The luminescence peak due to band-to-band electron–hole pair recombination is beyond the range of our detection system. The PL spectra are scanned from 550 to 800 nm with a GaAs detector and from 800 to 1700 nm with a Ge detector. Figure 1a displays only the red PL peak near about 650 nm. The red PL of the CdS colloidal particles arises from the existence of the sulfur vacancy V_S; according to the scheme shown by the inset in Figure 1a, the recombination process is[22,23]

$$CdS + h\nu \rightarrow CdS(h_{VB^+} + e_{CB^-}) \quad (1)$$

$$h_{VB^+} + e_{CB^-} \rightarrow h\nu_0 \quad (2)$$

$$h_{VB^+} + V_S \rightarrow V_{S^+} + h\nu_1 \quad (3)$$

$$V_{S^+} + e_{CB^-} \rightarrow V_S \quad (4)$$

The subscripts VB and CB mean the valence band and conduction band, respectively. The electrons and holes are created by the Argon-laser photons, and then the electron is trapped into the V_{S^+} vacancy at first, and consequently recombines with the hole in the valence band to give the red photoluminescence with photon

(24) Spanhel, L.; Weller, H.; Fojtik, A.; Henglein, A. *Ber. Bunsen-Ges. Phys. Chem.* **1987**, *91*, 88.
(25) Haus, J. W.; Zhou, H. S.; Honma, I.; Komiyama, H. *Phys. Rev. B* **1993**, *47*, 1359–1365.
(26) Bethke, P. M.; Barton, P. B. *Am. Mineral.* **1971**, *56*, 2034–2039.

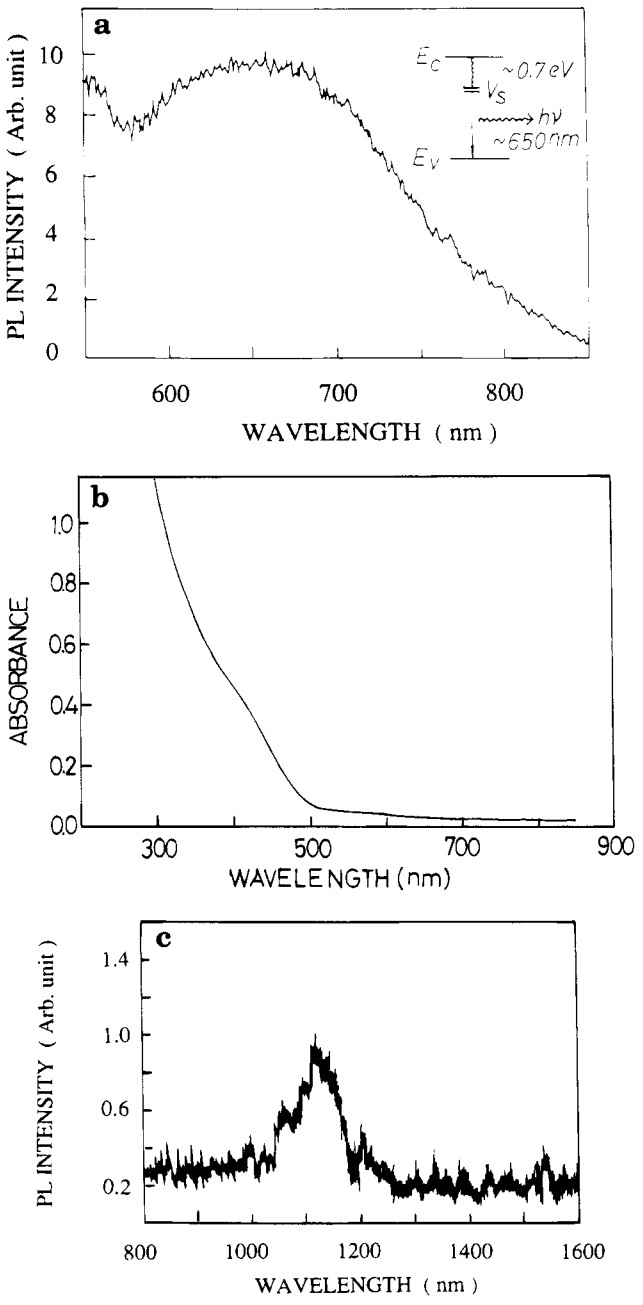

Figure 1. (a) Red PL spectrum of the CdS particles at room temperature. The insert shows a PL mechanism scheme of the CdS particles for this fluorescence; the electron capture is nonradiative. (b) Optical absorption spectrum of the CdS particles at the room temperature. The particle diameter is about 6 nm. (c) Feeble IR PL spectrum recorded from CdS particles. The PL spectrum peaks at about 1100 nm for our CdS particles.

energy $h\nu_1$ about 650 nm. The sulfur vacancy V_s is created as a luminescence center by surface kinetic processes during the synthesis.

We find that there is another PL peak for CdS particles in a near infrared range, which is shown in Figure 1c; it is very weak and the signal-to-noise is small. This PL peak has been reported[31,32] as Cd–S composite vacancies (V_{Cd-S}) in the CdS bulk crystal materials. It is an acceptor vacancy PL center.[31,32] The energy level for the ionization is located about 1.2 eV above the valence band.[31,32]

For the PbS nanoparticles, some groups find that the PbS nanoparticles prepared with a different stabilizer such as acetonitrile, zeolites, and polymer show very different optical properties.[27] Recently, the fluorescence spectra of PbS nanoparticles have been reported[28] in the visible (from 600 to 800 nm) range. However, we do not observe any PL spectra of PbS prepared with PVP as stabilizer in the wavelength range from 550 to 1700 nm. So, we consider only the PL spectra result from the vacancy emission of the CdS material.

Photoluminescence Spectra of CdS/PbS. *Photoluminescence Spectra of CdS Modified by Pb Cation.* When a small quantity of $Pb(CH_3COO)_2$ solution is injected into the CdS colloidal solution stated above, the surface of the CdS particles is modified by the Pb^{2+} ions. Figure 2 shows the absorption and PL spectra of the CdS colloidal nanoparticles modified by Pb^{2+} ions as the quantity of the $Pb(CH_3COO)_2$ solution added. The absorption results show that the exciton shoulder of the CdS colloidal solution disappears after adding the $Pb(CH_3COO)_2$ solution, although the absorption edge remains unchanging. The reason of the exciton shoulder disappearing is unknown.

Figure 2b shows that the PL spectrum that results from recombination of S vacancy and hole at 650 nm is quenched by the Pb cation surface modification. The PL intensity of the CdS can be reduced to half by adding the Pb cations in only a hundredth Pb/Cd molar ratio and almost entirely quenched by adding about a tenth.

Several researchers also report that the PL spectra of the semiconductor nanoparticles[18,29] are quenched by the transfer of carriers from the semiconductor nanoparticles to the surface layer.[22] A simple calculation shows that a surface layer can scarcely be formed when a molar quantity of Pb cation of only a hundredth or fiftieth of the amount of Cd atoms is added. So, we considered two plausible mechanisms: one is the formation of PbS islands on the CdS surface,[30] and the other is that the Pb cations bind to the sulfur atoms on the surface to quench the V_s defect center. The second case includes a Pb cation replacing a Cd atom in the neighbor of a V_s vacancy on the interface between CdS and PbS to quench the V_s photoluminescence center. The V_{Cd-S} growth mechanism will be discussed in a latter section.

The PL spectra in Figure 2c of CdS modified by Pb cations show that the recombination of a Cd–S composite vacancy and an electron emits a photon at 1100 nm and that the intensity is enhanced by the surface modification. The intensity increases, but the location of the peak does not shift for the Pb/Cd molar ratio in the range from 0.05 to 0.5.

Photoluminescence Spectra of CdS/PbS Coated Nanoparticles. As the quantity of Pb cations increases further, not only does the luminescence peak at 650 nm disappear but concurrently the PL of V_{Cd-S}, which appears in the near infrared range, increases in intensity and shifts to longer wavelengths. For a Pb/Cd molar ratio of 1.0, the intensity reaches a maximum. For such larger Pd/Cd molar ratios, we consider the particles to be coated. Figure 3a shows that the absorbance for larger cation ratios strongly shifts to

(27) Gallardo, S.; Gutierrez, M.; Henglein, A.; Janata, E. *Ber. Bunsen-Ges. Phys. Chem.* **1989**, *93*, 1080–1090.
(28) Nenadovic, M. C.; Comor, M. I.; Vasic, V. Micic, O. I. *J. Phys. Chem.* **1990**, *94*, 6390–6396.
(29) Weller, H.; Koch, U.; Gutierrez, M.; Henglein, A. *Ber. Bunsen-Ges. Phys. Chem.* **1984**, *88*, 649.
(30) Rossetti, R.; Brus, L. *J. Phys. Chem.* **1982**, *86*, 4470–4472.

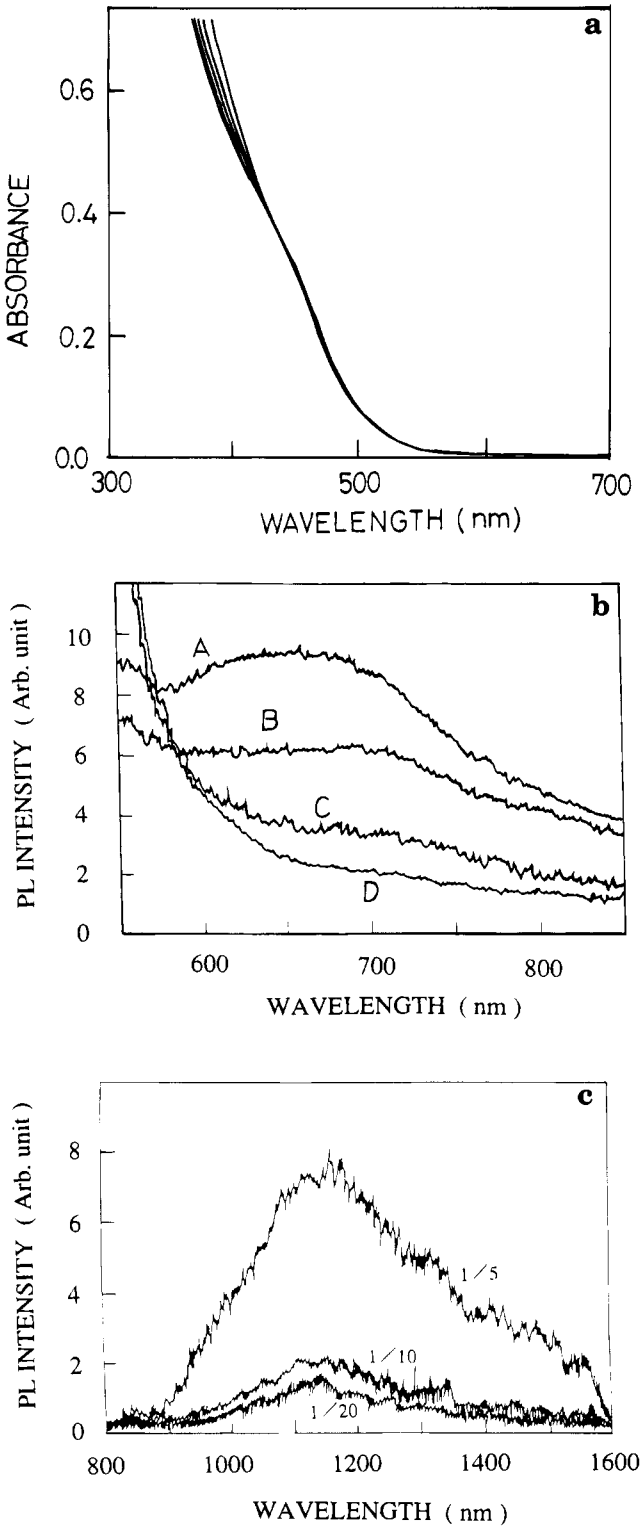

Figure 2. (a) Optical absorption spectrum of the CdS at room temperature after adding the small amounts of $Pb(CH_3COO)_2$ with the Pb/Cd molar ratios of 1/100, 1/50, 1/20, and 1/10 to the CdS nanoparticle colloidal solution; for wavelengths longer than 500 nm no change was observed and the shoulder moves from left to right in the figure with increasing molar ratios. (b) PL spectra of the CdS at room temperature after adding the some $Pb(CH_3COO)_2$ with the Pb/Cd ratio of 1/100 (B), 1/50 (C), and 1/10(D) to the CdS nanoparticle colloidal solution. Curve A is data without addition of Pb cations. If the Pb/Cd mole ratio is more than 1/10 the PL peak at about 650 is almost fully quenched. (c) Infrared PL spectra of the CdS/PbS coated particles at room temperature with Pb/Cd ratio in 1/20, 1/10, and 1/5 at about 1100 nm; the peak intensity increases as Pb/Cd molar ratio increases.

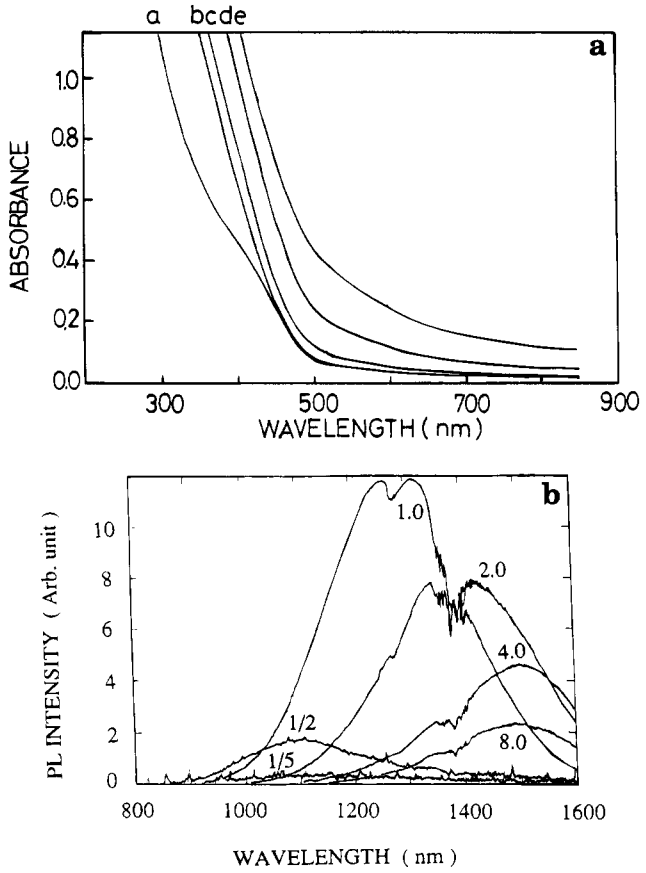

Figure 3. (a) Optical absorption spectra of the CdS/PbS-coated nanoparticles at room temperature with Pb/Cd ratio in $^1/_2$ (b), 1 (c), 2 (d), and 4 (e); curve a is the CdS absorbance without addition of Pb cations. The spectrum is taken 5 min after the injection of Pb cations into the CdS colloid solution. (b) PL spectra of the CdS/PbS coated particles with Pb/Cd ratio in $^1/_5$, $^1/_2$, 1, 2, 4, and 8 in the infrared range at the room temperature. The PL peak shifts from 1100 to 1500 nm as the molar of Pb/Cd increases from $^1/_5$ to 4. The spectrum is taken 5 min after the injection of Pb cations into the CdS colloid solution.

longer wavelengths. This trend is also observed in our previous publication.[20] The absorption edge shifts toward longer wavelengths as the molar ratio of Pb/Cd increases. This means that the bandgap of the CdS/PbS coated nanoparticles decreases as the thickness of the PbS shell layer increases.[20,25]

We find that the PL spectra of V_{Cd-S} shifts from 1100 to 1500 nm as the molar ratio Pb/Cd increases from 0.05 to 4.0, as is shown in Figure 3b. The large shift of the PL peak is correlated with the band edge shift deduced from the absorbance in Figure 3a. The data for the PL peak photon energies and the bandgap energy deduced from the absorption data are plotted in Figure 4a; it displays the correlation between the two quantities.

Infrared Photoluminescence. *Photoluminescence Peak Shift and Intensity.* When a Cd ratio in the CdS is exchanged by a Pb cation and migrates across the PbS shell layer into the solvent, defects and vacancies can also be created at the interface by the kinetic exchange process and strains induced by the lattice mismatch between the two materials. The defects become new PL centers at the interface in the CdS/PbS system. The Cd−S composite vacancy (V_{Cd-S}) is similar to an acceptor vacancy PL center.[32] The energy level for the ionization is located at about 1.2 eV above the

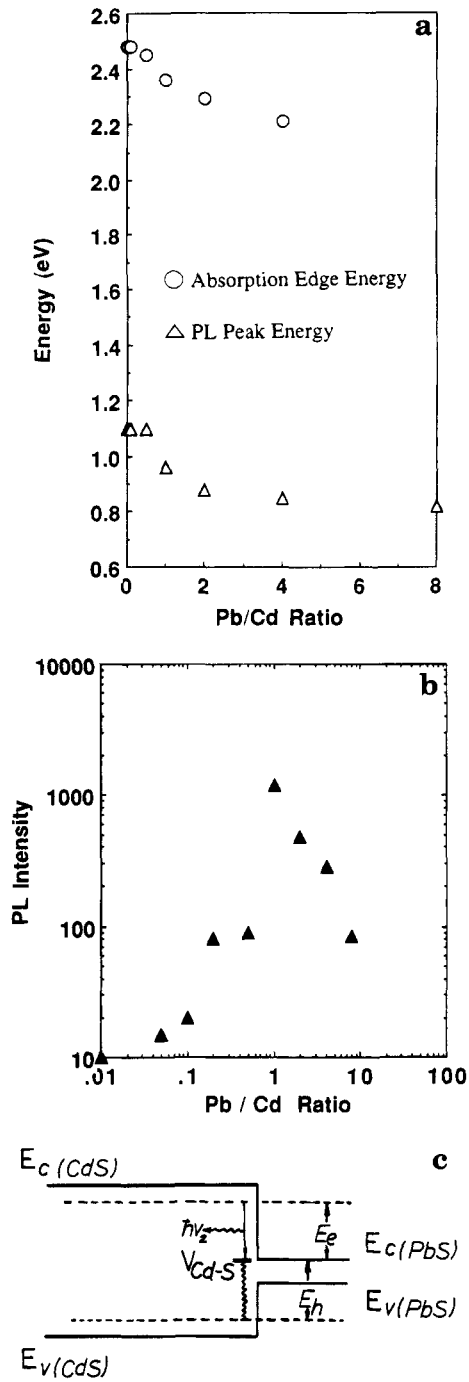

Figure 4. (a) Relationship between the absorption edge energy and the PL peak energy and the Pb/Cd molar ratio. (b) Relationship between PL intensity in infrared range and the Pb/Cd ratio. (c) Potential and the location of the vacancy in the CdS/PbS coated nanoparticles.

valence band.[31,32] This is the source of the infrared PL peak energies plotted in Figure 4a; the shift and variation of the peak intensity are given in figure 4(b).

The photoluminescence center for the red fluorescence is identified as the S vacancies, and the infrared PL center is the Cd−S composite vacancies. The S vacancy is reduced as the surface changes to a PbS layer, and at the same time, Cd−S composite vacancy increases due to the ion-exchange process. The radius of a Pb ion is bigger than that of a Cd ion, and furthermore the crystalline structure of PbS is different from that of CdS. The difficulty in the replacement of a Cd ion with Pb ion for these reasons may be responsible for the creation of the V_{Cd-S} composite vacancy as the Pb ion replacing a Cd atom adjacent to a V_S vacancy on the interface. So, such V_S vacancy becomes a V_{Cd-S} composite vacancy during the synthesis. This model can explain the experimental results of quenching of the red luminescence and increasing of the infrared luminescence.

We assume that the infrared PL of the CdS/PbS, which results from the V_{Cd-S} composite vacancy locates at the interface between the two semiconductor materials. The V_{Cd-S} composite vacancy is an acceptor type vacancy.[32] Figure 4c is a schematic of the band structure for the coated CdS/PbS nanoparticles including the recombination defect center. The bandgap of CdS core is larger than that of PbS shell layer. The subband state, shown as a dashed line, can lie below the conduction band edge of the CdS. The process from carrier excitation to recombination is

$$\mathrm{CdS/PbS} + h\nu \rightarrow \mathrm{CdS/PbS}(h_{VB^+} + e_{CB^-}) \quad (5)$$

$$e_{CB^-} + V_{Cd-S} \rightarrow V_{Cd-S^-} + h\nu_2 \quad (6)$$

$$V_{CD-S^-} + h_{VB^+} \rightarrow V_{Cd-S} \quad (7)$$

The electrons and holes are excited into an available subband state by an Argon laser, then the holes are trapped into the V_{Cd-S} composite vacancy acceptor through a nonradiative process, and recombine with the electrons in the excited electron level LUMO (1S level denoted by E_e) to give the infrared PL $h\nu_2$ through an radiative process. E_e is measured with respect to the bottom of the PbS conduction band. The bandgap of CdS is taken to be 2.4 eV, while the conduction band offset between CdS and PbS is 1.2 eV. Therefore, the valence band offset is 0.8 eV. Because the E_e also decreases as the core/shell ratio increases, the gap between the E_e and the $E(V_{Cd-S})$ vacancy level also decreases (red shift) as the shell/core ratio increases. The energy of the PL photon is

$$h\nu_2 = E_e + E(V_{Cd-S}) \quad (8)$$

and $E(V_{Cd-S}) = 0.0$ eV.

A quantum confinement model can be used to correlate the energy shift with the PL emission. The trends found for the PL emission peak shift in Figure 4a can also be correlated with the shift of the absorption edge.

The optical bandgap is determined by an extrapolation at a high-energy side of the absorption slope from the Figure 3a. The reason is that the low-energy absorption comes from both scattering and absorption of some separated PbS nanoparticles in the solution. A plausible origin of the scattering is from the formation of a colony of the particles (aggregates) by salting out in the high Pb ion concentration. Also, some small PbS particles should be stripped off from the surface of the coated nanoparticles, and these particles have absorption in the longer wavelength region.

(31) Sheinkman, M. K.; Ermolovich, I. B.; Belen'kii, G. L. *Soviet Phys., Solid State* **1969**, *10*, 2069−2076.
(32) Susa, N.; Watanabe, H.; Wada, M. *Jpn. J. Appl. Phys.* **1976**, *15*, 2365−2370.

Although we have not determined the relationship between thickness of the shell layer and the Pb/Cd molar quantity in the aqueous solution, there is a correspondence between the Pb/Cd ratio and the thickness of the shell layer.

Figure 4b shows the relationship between the PL intensity in infrared range and the Pb/Cd molar ratio. We find that the PL intensity in infrared range increases very slowly at first but then very rapidly after the 680 nm peak was completely quenched. For large molar ratios the peak vanishes due to the small core of CdS in these particles.

Model Calculation. Nanometer size semiconductor particles coated with another semiconductor can exhibit unusual and interesting phenomena associated with the redistribution of the electron and hole wave functions. A theoretical calculation of the excitation energy of the coated heterostructure semiconductor particle has been reported in our previous publication,[25] as well as by other groups. Experimental results on heterostructure particles have also been examined in the context of the quantum-size effects.[20,33]

The theoretical analysis starts with the effective mass approximation with single bands for both the conduction and valence-band carriers. The particle has an outer radius R, and the interface between the core and the shell layers has a radius a. The single envelope wave functions are used in each band. We assume strong confinement, where the Coulomb interaction between the carriers can be neglected in comparison with the confinement energies. The Schrodinger equation and the wave function can be written as

$$\left[-\frac{h^2}{2}\nabla\cdot\frac{1}{\mathrm{m}_\alpha(\mathrm{r})}\nabla + V_\alpha(r)\right]\psi_\alpha = E_\alpha\psi_\alpha \qquad (9)$$

where α(= e or h) used as a subscript denotes the electrons or the holes. The potential in the core is

$$\mathbf{V}_\alpha(\mathrm{r}) = \mathbf{V}_\alpha{}^{\mathrm{c}}; \qquad 0 \le r \le a \qquad (10a)$$

and the potential in the shell is

$$\mathbf{V}_\alpha(r) = \mathbf{V}_\alpha{}^{\mathrm{s}}; \qquad a \le r \le R \qquad (10b)$$

Outside the shell, the potential is assumed to be infinite. The effective mass in the core material also differs from the effective mass in the shell material. The wave function is divided into two parts; in the core region it is

$$\psi_\alpha{}^{\mathrm{c}}(r) = A_\alpha{}^{\mathrm{c}} j_0(k_\alpha{}^{\mathrm{c}} r); \qquad 0 < r < a \qquad (11a)$$

and the shell region form is

$$\psi_\alpha{}^{\mathrm{s}}(r) = A_\alpha{}^{\mathrm{s}} j_0(k_\alpha{}^{\mathrm{c}} r) + \mathrm{B}_\alpha{}^{\mathrm{s}} n_0(k_\alpha{}^{\mathrm{s}} r); \qquad a \le r \le R \qquad (11b)$$

The superscripts c and s on the wave functions denotes the core or shell range. Here we only consider the 1S subband state; $j_0(r)$ and $n_0(r)$ are the spherical Bessel and Neumann function, respectively. The coefficient in the argument is (the superscript β denotes the core and shell regions)

$$k_\alpha{}^\beta = \sqrt{2(E_\alpha - V_\alpha{}^\beta)/m_\alpha{}^\beta h^2} \qquad (12)$$

At the shell boundary, a, the continuity of the wave function and the normal component of the probability current give the following relations:

$$\psi_\alpha{}^{\mathrm{c}}(a) = \psi_\alpha{}^{\mathrm{s}}(a) \qquad (13a)$$

$$\frac{\mathbf{n}}{m_\alpha{}^{\mathrm{c}}}\cdot\nabla\psi_\alpha{}^{\mathrm{c}}(\mathbf{r}) = \frac{\mathbf{n}}{m_\alpha{}^{\mathrm{s}}}\cdot\nabla\psi_\alpha{}^{\mathrm{s}}(\mathbf{r}); \qquad \mathbf{r} = a \qquad (13b)$$

where $\mathbf{n}$ denotes the unit vector normal to the surface. The shell wave functions vanish at the outer boundary.

The band offsets, giving the values for $\mathbf{V}_\alpha{}^{\mathrm{c}}$ and $\mathbf{V}_\alpha{}^{\mathrm{s}}$ in the model, and the effective masses have been discussed in our previous paper.[25] We use a conduction band offset between the CdS and PbS materials of 1.2 eV. The masses of the electrons and holes in each material are $m_{\mathrm{e}}(\mathrm{CdS}) = 0.2m_0$, $m_{\mathrm{h}}(\mathrm{CdS}) = 0.7m_0$, $m_{\mathrm{e}}(\mathrm{PbS}) = 0.08m_0$, $m_{\mathrm{h}}(\mathrm{PbS}) = 0.075m_0$ and m_0 is the electron mass in free space. The radius of the particle is taken to be 2.5 nm. The bandgap energy of the bulk CdS material is 2.4 eV. The energies of the E_{e} and E_{h} are the lowest available energy levels of the electron and hole, respectively. The bandgap energy is not only dependent on the size of the coated nanoparticles but also strongly dependent on the core-shell ratio a/R. The coated nanoparticles are considered to be coherent over the whole particle when we deal with the electrons and holes in this sytem. This is equivalent to treatments of subband states in semiconductor superlattices.

Figure 5a is a plot of the excited energy bandgap (HOMO−LUMO), $E = E_{\mathrm{e}} + E_{\mathrm{h}}$, and the electron energy shift, $E_{\mathrm{e}} + V_{\mathrm{Cd-S}}$, versus the ratio of the core thickness to the shell radius $(R - a)/R$. The theoretical results for the electron energy shift, which corresponds to the infrared fluorescence peak, $h\nu_2$, from eq 8, is also shown in Figure 5a. It also decreases in energy as the shell layer increases, but by a smaller amount.

Comparison of Figure 5a and Figure 4a reveals that the trend of the energies for the model correspond to the absorption band edge energy and the PL peak position. There are, however, quantitative differences, especially for the CdS-rich particles; the variation of the energies over the range of core/shell ratios is larger than those observed in the experiment. This is to be expected, considering the simplicity of the model; there are two improvements that are necessary in the model, which will also improve the agreement: the Coulombic effects, which include the interaction between the carriers and medium polarization induced by the finite height of the barrier between the shell and the host material. Both tend to lower the energy in the CdS particle but have little effect on the PbS particle. Coulombic effects depend upon the dielectric constant of the material, which is 11 for CdS and 185 for PbS. This effect is expected to lower the subband energies by about 10% for CdS particles and is negligible for the PbS particles;[33] the finite barrier height also affects the CdS particles more than the PbS particles because the bandgap is much larger for the CdS than for PbS; the

(33) Sharkin, V. A.; Hanamura, E., preprint.
(34) Hasselbarth, A.; Eychmuller, A.; Eichberger, R.; Giersig, M.; Mews, A.; Weller, H. *J. Phys. Chem.* **1993**, *97*, *5333–5340.*
(35) Eychmuller, A.; Hasselbarth, A.; Weller, H. *J. Lumin.* **1992**, *53*, *113–115.*
(36) Eychmuller, A.; Mews, A.; Weller, H. *Chem. Phys. Lett.* **1993**, *208*, 59–62.

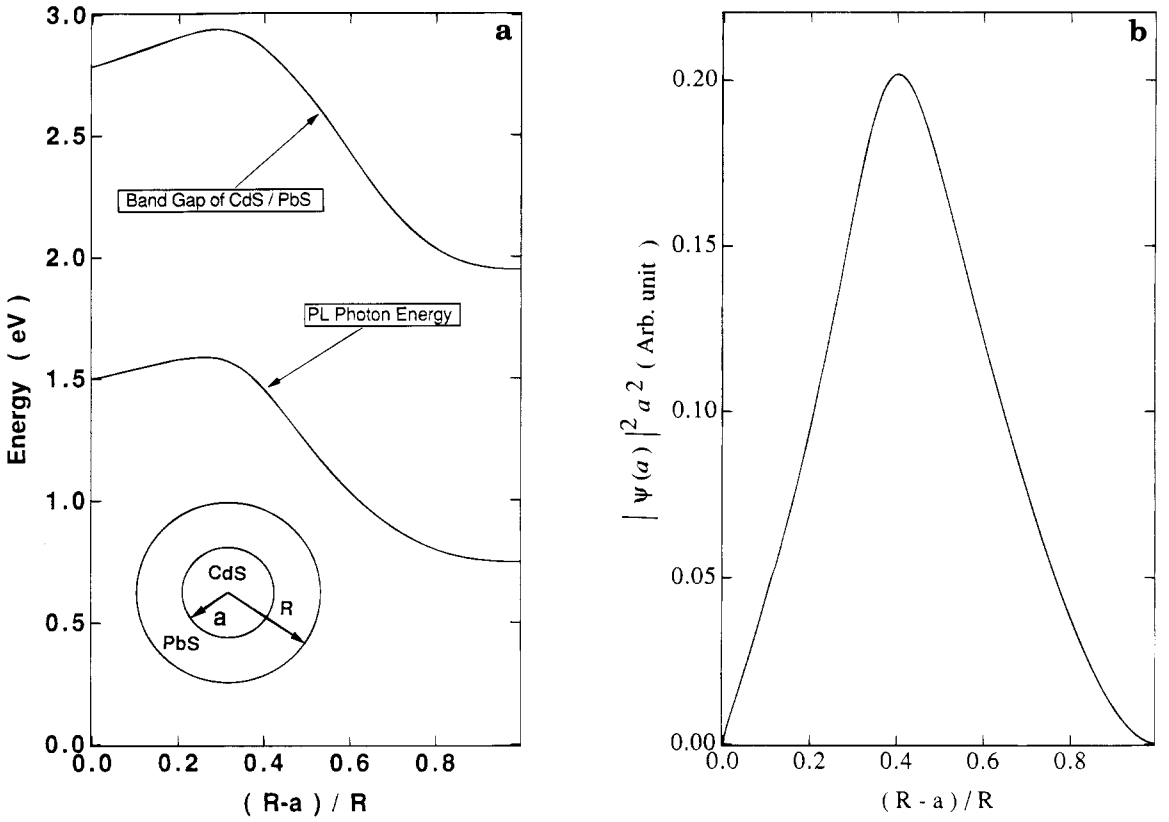

Figure 5. (a) Curve 1 shows the excited energy gap (from 1S electron state to the 1S hole state) of the CdS/PbS versus the shell thickness to shell radius ratio, $(R - a)/R$, calculated in the effective mass approximation. The excited energy gap is depend on not only the size of the coated nanoparticles but also the core/shell ratio. Curve 2 shows the energy difference between the 1S electron state and the defect state, which also depends on the ratio defined above. To aid the reader, a schematic figure of a particle with a CdS core and a PbS shell is shown. (b) Theoretical determination of the PL intensity dependence on the ratio of the shell thickness to the shell radius.

barrier height depends on the host material in which the particles are embedded.

It has been pointed out above that the absorption data were taken from the sample in the solution. According to the thermodynamics, the volume fraction of the shell layer in the dried sample may become larger as the reaction ($CdS + Pb^{2+} \rightarrow Cd^{2+} + PbS$) proceeds, and, in that case, the bandgap should become smaller. Although we have not checked the exact composition of the dried sample, the correspondence between the theoretical prediction about the bandgap and PL energy and experimental results will be better if we exactly know the growth of the PbS shell layer induced by drying.

But the difference in the composition does not alter the transient behavior of the bandgap, the PL energy, or the basic treatment of the quantum size properties of the core/shell particles. The difference between the experimental results and the theoretical calculation is small.

Also, the intensity of the PL peak can be estimated by our model. The defects are at the interface, and the PL intensity depends on the number of defects and the electron density at the core/shell interface. We assume that the density of defects at the interface is constant with the core/shell radius; the PL peak intensity is thus proportional to

$$I_{PL} \sim |\psi_e(a)|^2 a^2 \qquad (14)$$

The PL vanishes as a approaches zero; however, it also becomes small as a approaches R, since the wave function vanishes at the shell boundary. We find the maximum of the PL intensity in this model occurs around $a \approx 0.6R$.

Table 1. Photoluminescence and Absorption Data Comparison with Model Calculations[a]

		$h\nu_2$ (eV)		energy gap (eV)	
Pb/Cd ratio	$(R - a)/R$	exp	theory	exp	theory
1	0.4	0.96	1.45	2.36	2.8
2	0.65	0.88	0.95	2.28	2.3
4	0.75	0.85	0.80	2.20	2.1
8	0.88	0.82	0.75		1.9

[a] The second column is deduced from Figure 5b after the intensity data has been scaled.

The plot of the peak intensity versus the shell thickness to shell radius ratio is shown in Figure 5b. The experimental PL peak intensities in Figure 4b can be correlated with those in Figure 5b to infer a value for the core/shell ratio; for instance, when the maximum PL peak intensity is assumed to correspond to the curve maximum in Figure 5b, we find the ratio of the shell thickness to shell radius is 0.4. From this information the PL photon energy from Figure 4a can be compared with that in Figure 5a. This has been done in Table 1 for molar ratios larger than unity; the experimental PL peak intensities are simply scaled relative to the maximum value, and their corresponding relative value in Figure 5b yields the core/shell ratio. The ratios of shell thickness to shell radius are given in the second column of the table. The PL peak photon energy and the band edge energy are compared directly using Figures 4a and 5a.

We note that the agreement between the model and the experiment is satisfactory given the shortcomings of the model discussed above. Our choice of particle radius, 2.5 nm, is smaller than observed in TEM photographs; the TEM data indicate a radius of 3 nm. No attempt has been made at this point to provide a better fit to the data, for instance, by including Coulombic effects, which would lower the energies for the smaller Pb/Cd molar ratios by about 0.2 eV.[33] Attempts to directly record the core/shell ratio by high-resolution TEM have not been successful. Further investigations, both theoretical and experimental, are required in order to draw more quantitative conclusions.

Conclusion

The PL spectra from colloidal solutions of the coated CdS/PbS nanoparticles system have been investigated at room temperature. The PL spectra of CdS/PbS-coated nanoparticles appear in the wavelength range from 1100 to 1500 nm and shift to longer wavelength as the quantity of the Pb cation increases. We discuss the role of Cd−S composite vacancy PL center in the CdS/PbS system and calculate the energy gap from the electron excited level (LUMO) to Cd−S composite vacancy level by the effective-mass model. The value, just as the excited energy gap in the CdS/PbS system, not only is dependent on the size but also strongly depends on the core/shell ratio. The theoretical results are comparable with the PL results in general. Namely, the red shift and the intensity maximum of the PL spectra with increasing shell layer can be explained by the radiative transition of an electron from the 1S electron quantum state to the V_{Cd-S} vacancy state on the core/shell interface of the coated CdS/PbS system.

Some simple theoretical models have been successfully applied to layered heterostructures in the past, but no such analysis coupled with experiment had been attempted for heterostructure particles. Although these techniques need refinement to be quantitative, they can be applied to other systems to provide the correct quantitative features of the carriers dynamics. Future studies should be devoted to examining the electron and hole dynamics to determine the validity of this modeling technique. The addition of Coulomb and polarization effects also certainly alter the results somewhat and need to be evaluated before a competitive quantitative analysis can be attempted. The main difficulty to be overcome in directly comparing the theory to the experimental results is in an experimental determination of the core/shell ratios. Attempts in this direction have been made without success, so far. Future studies will attempt to solve this difficult experimental problem.

Heterostructure-coated nanoparticles can be used to obtain new information about the material properties. The defects at the interface can be probed by luminescence spectroscopy and add a new dimension to studies of the carrier dynamics. New physical phenomena can also be expected in these particles; for instance, since the electron and hole wave functions no longer overlap, there is a static electric field generated within the nanoparticles due to the charge separation. Because of the small size of the nanoparticles, the static field can be quite large and stark shifts of spectral features can be expected.

Acknowledgment. We are grateful to Prof. E. Hanamura (Department of Applied Physics, the University of Tokyo) for helpful comments and suggestions, as well as Dr. K. Kawanami (National Electrotechnique Laboratory, Tsukuba, Japan) for generous access to his laboratory for the PL measurements. J.W.H. gratefully acknowledges the support and hospitality of the Research Center for Advanced Science and Technology of the University of Tokyo.